Pervasive and Mobile Computing 79 (2022) 101511

Contents lists available at ScienceDirect

Pervasive and Mobile Computing

journal homepage: www.elsevier.com/locate/pmc

Review

Spectrum cartography techniques, challenges, opportunities, and applications: A survey

Yeduri Sreenivasa Reddy [a], Abhinav Kumar [b], Om Jee Pandey [c], Linga Reddy Cenkeramaddi [a,*]

[a] ACPS Group, Department of Information and Communication Technology, University of Agder, Grimstad, Norway
[b] Department of Electrical Engineering, IIT Hyderabad, Hyderabad 502285, India
[c] Department of Electronics Engineering, IIT BHU Varanasi, Varanasi 221005, India

ARTICLE INFO

Article history:
Received 5 March 2021
Received in revised form 7 September 2021
Accepted 16 November 2021
Available online 3 December 2021

Keywords:
Channel gain map
Channel state information
Interference map
Mean absolute error (MAE)
Mean square error (MSE)
Normalized MSE (NMSE)
Power spectral density map
Power map
Radio frequency (RF) power
RF map
Root MSE (RMSE)
Spectrum cartography
Spectrum map
Transmitter locations

ABSTRACT

The spectrum cartography finds applications in several areas such as cognitive radios, spectrum aware communications, machine-type communications, Internet of Things, connected vehicles, wireless sensor networks, and radio frequency management systems, etc. This paper presents a survey on state-of-the-art of spectrum cartography techniques for the construction of various radio environment maps (REMs). Following a brief overview on spectrum cartography, various techniques considered to construct the REMs such as channel gain map, power spectral density map, power map, spectrum map, power propagation map, radio frequency map, and interference map are reviewed. In this paper, we compare the performance of the different spectrum cartography methods in terms of mean absolute error, mean square error, normalized mean square error, and root mean square error. The information presented in this paper aims to serve as a practical reference guide for various spectrum cartography methods for constructing different REMs. Finally, some of the open issues and challenges for future research and development are discussed.

Contents

* Corresponding author.
E-mail addresses: sreenivasa.r.yeduri@uia.no (Y.S. Reddy), abhinavkumar@ee.iith.ac.in (A. Kumar), omjee.ece@iitbhu.ac.in (O.J. Pandey), linga.cenkeramaddi@uia.no (L.R. Cenkeramaddi).

https://doi.org/10.1016/j.pmcj.2021.101511

1. Introduction

The growth in the usage of radio frequency based communication services increases the challenges in accessing the spectrum [1]. Further, ever-increasing number of wireless devices causes spectrum crowding and results in the frequent use of frequency links (channels). In such cases, intelligent methods such as spectrum cartography (SC), also known as radio environment map (REM) are essential to utilize the spectrum resources effectively. The SC constructs a map from the channel parameters collected from the sensor nodes deployed in a certain geographical area. The corresponding channel parameters can be received signal power or channel gain (CG) or power spectral density (PSD) [2,3].

Cognitive Radio (CR) is one of the technologies that benefit from REM due to the usage of dynamic spectrum access. CR allows the secondary users (SUs) to access the resources that are not utilized by primary users (PUs) without causing any interference to PUs. Thus, these users need to be aware of the channel conditions in order to make the intelligent decisions [4], which then helps in controlling the interference caused by secondary network to the PUs that are not transmitting [5,6]. Thus, construction of REM helps the SUs to know the channel conditions. It allows them to utilize unused spectrum without causing interference to PUs. REM also supports various CR applications such as spectrum access in license band, spectrum sharing in unlicensed band, radio resource management, and spectrum monitoring [7].

A recent use case for REMs is in unmanned aerial vehicles (UAVs) communications have gained significant attention as they can be used as flying relays for wireless networks. One of the applications of UAVs is to deploy them at low altitude to provide superior link quality to users in dense urban environment with deep shadow fading. However, such an application requires the knowledge of the channel conditions between the UAV and ground station. Therefore, it is essential to learn the channel conditions of UAV–user pair. Thus, REM helps in constructing the radio map between all possible locations of UAV–user pair [8].

Another scenario is the use of television (TV) spectrum for data delivery. The TV bands can be used by SUs without causing any degradation in the quality of service requirements of incumbent users operating inside the building or nearby. This is possible when the SUs have access to the knowledge about the PUs activities. The REM helps the SUs to have complete knowledge on the radio activities of PUs [9].

Extreme doppler shifts are common in high speed trains (HSTs) and are detrimental to the orthogonal frequency division multiplexing (OFDM) based LTE-Railway system. Further, the existing Doppler shift estimation methods do not consider the features of HST such as the regular train routes, time tables, and predictable train routes for channel estimation. The REM construction methods which are discussed in this article provide the detailed view on these features [10]. Future 5G enables the vehicles to communicate with each other as well as with the infrastructure through vehicle-to-anything (V2X) communication. However, the channel model changes when the vehicle moves from one location to another and the variation is high in urban scenarios. The REM can help in estimating the channel quality which helps us to adapt the resources of a vehicle heading to a poor coverage area.

In this survey, the functional architecture of REM, various types of REMs, and the performance metrics used for the evaluation of SC algorithms are first discussed. Then, we describe the state-of-the-art mechanisms for the construction of various REMs focusing on machine learning based approaches. We present the performance analysis of nearest neighbor (NN) method for the construction of REMs in order to provide better insights of SC. In this method, the REM at a location is estimated as the REM of a node which is nearest to the location. The numerical results are presented with single REM measuring unit and three REM measuring units. Subsequently, the performance is evaluated in terms of mean absolute error (MAE), mean square error (MSE), normalized MSE (NMSE), and root MSE (RMSE).

The rest of the paper is organized as follows: An overview of the SC is presented in Section 2. The state-of-the-art SC mechanisms are discussed in Section 3. The performance comparison of state-of-the-art mechanisms is discussed in Section 4. Finally, we provide the concluding remarks with a possible future work in Section 5.

2. Overview of spectrum cartography

REM defines the radio environment in different domains such as radio regulations, terrain information, and radio frequency (RF) emission. It maintains the information about radio elements, radio scene, and environment. In general, REM is constructed from the sensor node data. Thus, it can be easily adapted to dynamic environmental conditions. In [11], an overview of the REM architecture, construction techniques, and quality metrics have been discussed. It is then extended to heterogeneous networks composed of both licensed and unlicensed bands in [12]. Moreover, it has been extended in [13,14] to cellular networks in the presence of heterogeneous LTE networks comprising of macro cell and femto cells. A survey on the REM architecture for 5G cognitive radio networks (CRNs) has been presented in [15].

REM construction architecture involves four entities as shows in Fig. 1. Initial block represents the sensor nodes need to be deployed to collect the information and send it to the REM data storage and acquisition unit, which stores the

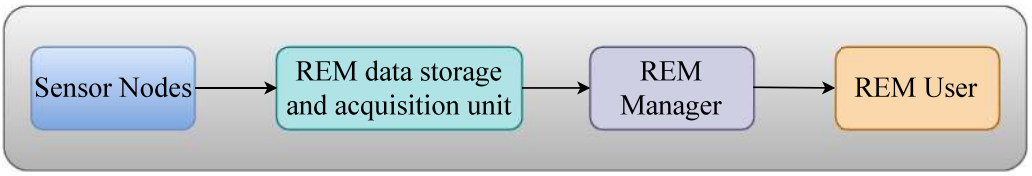

Fig. 1. Functional Architecture of REM.

sensor data and other processing information. The subsequent block indicates the REM manager which processes the data collected by REM data storage and acquisition unit and constructs the REM. Once REM is constructed, SUs access the unused resources for information transmission as depicted in the fourth block in Fig. 1 [12].

Based on the collected information, REM is categorized as channel gain (CG) map, power spectral density (PSD) map, power map, spectrum map, power propagation map, radio frequency map, or interference map. The CG map constructs the map that provides the channel state information between any two locations over a given link. Spectrum map aims at constructing the received signal power from one location to another location over a given frequency band. Spectrum map is also referred as RF REM. Interference map generation requires the measurement of the field strength at every location of interest. REM constructed from the sensor node measurements provides the channel state information for links between all locations even though sensors are not present. This helps in the network planning and interference management in cellular networks [16]. From the state-of-the-art, we notice that the construction of power map, CG map, and frequency map are at most focused. Thus, we have highlighted the construction of these maps in this manuscript.

With P_0 denoting the received power at reference distance $d_0 = 1$ m and α being the pathloss exponent, the received power P_r (in dB), at a distance d, for the construction of power map is defined as [17]

$$P_r = P_0 - 10\alpha \log_{10}\left(\frac{d}{d_0}\right). \tag{1}$$

Further, the CG at a distance of d for the construction of CG map is given as [18]

$$\gamma(dB) = \beta(dB) - 10\alpha \log_{10} d + \zeta\,, \tag{2}$$

where, β, α, and ζ denote the average CG at reference distance $d_0 = 1$m, path loss exponent, and shadow fading. ζ can be usually modeled as the zero mean Gaussian random variable with variance of σ^2. Finally, the frequency map can be obtained by finding the received signal power from each user to BS at each frequency. The expression for received power, P_r, at a distance d is given as

$$P_r = P_t - 21.98 + 20\log_{10}(\lambda) - 20\log_{10}(d)\,, \tag{3}$$

where, P_t denotes the transmitted power, d is the distance between each user and BS, and $\lambda = c/f$. Here, $c = 3 \times 10^8$ m/s denotes the light speed and f is operating frequency.

From REM, we can estimate the transmitter locations, RF power, and channel state information [5]. The efficiency of a REM construction algorithm is usually evaluated in terms of the construction time, number of sensor nodes considered for collecting data, and sensor node deployment. Further, the performance of any of the REM construction algorithm is evaluated in term of MAE, MSE, NMSE, or RMSE, which usually defines the error in reconstructing the REM. The expressions for MAE, MSE, NMSE, and RMSE, respectively, are obtained as

$$MAE = \frac{1}{n}\sum_{i=1}^{n} |x_i - \hat{x}_i|\,, \tag{4}$$

$$MSE = \frac{1}{n}\sum_{i=1}^{n} (x_i - \hat{x}_i)^2\,, \tag{5}$$

$$NMSE = \frac{E\left[(x_i - \hat{x}_i)^2\right]}{E\left[x_i^2\right]}\,, \tag{6}$$

$$RMSE = \sqrt{\frac{1}{n}\sum_{i=1}^{n} (x_i - \hat{x}_i)^2}\,, \tag{7}$$

where, n denotes the number of samples, x_i is the measured value of sample i and $\hat{x}_i$ is the reconstructed value, and $E[\cdot]$ denotes the expected value [1]. Finally, we can also estimate the transmitter locations, RF power, and channel state information from the reconstructed maps.

3. State-of-the-art mechanisms

In this section, we discuss the state-of-the-art mechanisms focusing on architecture, sensor node deployment, and REM construction. The consideration of number of sensor nodes, their locations, and way they collect the data has significant effect on the REM construction. Thus, we first discuss some of the literature focusing on the sensor node deployment. Then, we discuss the state-of-the-art REM construction methods. Most of the REM construction methods are compressive sensing based methods which reduce the number of samples need to be processed. Consequently, we discuss some of the machine learning (ML) based approaches in literature focusing on the construction of REM due to the diversity in the ML application.

3.1. Architecture

Crowdsourcing based web spectrum monitoring system has gained increasing popularity in recent times. It provides spectrum statics information to governmental organizations or telecom providers. However, the services does not reach to the layman that limits its widespread deployment. In order to address this, Electrosense+ has been presented in [19] that creates a open platform for spectrum sensing that uses low cost, embedded, and software defined spectrum IoT sensors. The architecture contains a predecessor and Elecrosense for controlling and monitoring the spectrum IoT sensors. Further, the authors have proposed different mechanisms to encourage the users to deploy new sensors for operating in the Electrosense network. Moreover, they have proposed a novel method of assigning a reward to encourage the users to host IoT sensors. Finally, a new Electrosense+ system architecture has been proposed to evaluate the performance for decoding wireless signals such as FM and AM radio, LTE, and ACARS. In [20], the authors have designed, implemented, and validated the hardware and software architectures for wideband radio spectrum monitoring inspired from the Lambda architecture. This system offers spectrum sensing services to end users to easily access and process the radio spectrum data. The authors have finetuned the data processing chain to reduce the latency of the services offered. The data models for MongoDB and Cassandra databases have been designed for analyzing the sensor data characteristics. For spectrum visualization, a MapReduce job has been developed and compared the performance of both the databases with experiments. It has been concluded that Cassandra database outperformed the MongoDB database when different types of queries applied on the data streams. A real time implementation solution for spectrum sensing using software defined radio USRP has been proposed in [21]. The proposed solution uses the energy levels and radio frequency data detected at the USRP to detect the spectrum occupancy. The hardware and software architectures of the proposed solution has been described thoroughly and the optimal configuration of the USRP platform is described for spectrum sensing.

3.2. Sensor node deployment

This section focuses on the number of sensor nodes deployed to collect the RSSI. In [22–24] the authors have discussed the effect of placement of sensor nodes and the selection of interpolation method on the REM constructed for very high frequency/ultra high frequency band scenarios. A new tool has been discussed in [25] to construct the power map using the RF power received from a set of sensor nodes deployed in a region of interest. The authors have used a data set that contains the real-world power measurements to obtain the path loss exponent and decorrelation time for the region of interest. Then, the power map is constructed using three interpolation techniques with a consideration of model-based and model-free approaches. Finally, the authors have obtained minimum number of measurements to accurately construct the map [25]. In [26], a novel distributed clustering (DC) algorithm has been proposed to construct the spatial interference maps with limited number of sensor node deployment. Here, the clusters are formed subsequently with limited number of sensor nodes with a constraint on Kriging variance. It has been shown that the proposed mechanism is performed in a distributed way is power efficient, low complex, and scalable to network size [26]. In [27], the authors have extended the DC algorithm by allocating the communication cost as a metric to decide which nodes are included in each cluster. Through extensive simulations, it has been claimed that the proposed mechanism improves the network lifetime by forming clusters of an average of 5 nodes only [27]. In [28], a SC technique has been proposed for CR where the fixed wireless sensor network (WSN) is deployed to support the CR terminals. In this technique, the WSN is deployed to estimate and update the PSD maps based on either centralized or distributed Kriging algorithm with the utilization of spacial correlation of PSD over a given area. It has been shown that the ordinary Kriging technique applied to SC outperforms the classical interpolation techniques with a proper semivariogram model even though the assumption of constant PSD is in general not fulfilled.

3.3. Compressive sensing based methods

In [29], compressive sensing multispectral cartography (CSMC) has been proposed for spectrum sensing that collects fewer samples than the required Nyquist criterion. Using collected samples, the method reconstructs the sparse or compressible signals. In [30], a SC algorithm has been proposed where the PSD maps are constructed from the highly quantized compressed measurements of wideband signals. In [31], REM has been formulated as a compressive sensing (l_1 minimization) problem that exploits the sparsity of the PUs in the space. Then, the Orthogonal Matching Pursuit

Table 1
Comparison of the compressive sensing based methods.

Method	Pros	Cons	Application/ Deployment scenario
CSMC [29]	(1) Reduced number of storage data (2) 50% data samples are sufficient to built multispectral data cube (3) 6.25% of original data is required to store the SC information	Requires transmitter locations and other information	(1) Smart cities (2) CSMC network
SC algorithm [30]	(1) Maps are constructed from the highly quantized compressed measurements of wideband signals (2) Consideration of simple wideband converters	(1) Requires transmitter locations and other information (2) Costly in terms of energy and bandwidth due to the requirement of spatially high density measurements	(1) Multipoint-to-point medium access topologies (2) IEEE 802.22
OMPSE [31,32]	30% improvement in the detection of wireless microphone in comparison to existing methods	Described how power is distributed spatially but not over frequency	TV White Space Wireless Microphone detection
Location-free SC method [33]	(1) Does not considers the locations of sensors (2) Overcomes the limitation of multipath affect on pilot signals	Feature have similar nature that of time of arrival (ToA) or time difference of arrival (TDoA) but not same	(1) Network planning (2) Power control (3) Cognitive radios
Coupled block-term tensor decomposition framework [34]	Guaranteed identifiability of the emitter radio map under realistic conditions	The assumption of spatial loss fields as low rank matrices could be violated in urban or indoor environments	For systematic and random sensor deployment
Non-parametric SC algorithm [35]	Comparable performance to semi-parametric methods	Described how power is distributed spatially but not over frequency	For systematic and random sensor deployment
Online SC method [36]	Reconstructs the PSD map in both space and frequency	(1) Requires transmitter locations and other information (2) Costly in terms of energy and bandwidth due to the requirement of spatially high density measurements	Cognitive radio

Spatial Extension (OMPSE) algorithm has been used to solve the compressive sensing problem. In [32], the authors have extended the work in [31] by considering fading environment in which the channel estimation is not feasible. In [32], the compressive sensing based approach has been investigated for SC in an urban environment where Rayleigh fading is prominent. Thus, the authors have formulated the cartography problem as a weighted l_1 norm minimization and an extension to the Iteratively Reweighted l1 (IRL1) algorithm has been used to solve the weighted l_1 norm minimization problem. Some of the existing SC techniques are required to estimate the locations of the sensor nodes. However, the multipath propagation, especially in urban scenario, affects the pilot signals used to estimate the location of the sensor nodes. Thus, in [33], a novel location-free SC method has been proposed which depends on the features of the pilot symbols rather than locations of the sensor nodes. Further, the authors have proposed kernel-based learning algorithm to explain the same. To address the disaggregation problem of the radio maps, a novel coupled block-term tensor decomposition framework has been proposed in [34]. Unlike the existing cartography methods, the proposed framework allows to recover the radio map of each transmitter. It has been claimed in [34] that the proposed framework works under a number of systematic and random sampling schemes. Thus, it allows the system designers to handle the situations where the sensor nodes deployment is challenging. The existing SC methods are parameter dependent such as transmitters location and other parameters need to be considered. Further, they also require spatially high density measurements which are costly in terms of energy and bandwidth. Motivated by this, in [35], the authors have developed a non-parametric SC algorithm where the lower density measurements are used to update the parameters of the basis functions. Here, the non-parametric means the parameters that are independent of the location and PSDs of the transmitters. An adaptive Gaussian radial basis functions (RBFs) with no prior knowledge of the transmitters have been suggested to achieve this goal. An online SC method has been proposed in [36] that reconstructs the PSD maps based on the compressed and quantized sensor measurements. PSD values at each location is decomposed into a linear combination of power spectra scaled by attenuation function which captures the propagation effects. Further, the attenuation function is represented as sum of two components, where the first one denotes the linear combination of a collection of basis function and the later denotes an element of a reproducing kernel Hilbert space of vector valued functions. Finally, the authors have proposed a novel stochastic gradient descent method to compute both the components in a online fashion [36]. A detailed description on each of the compressive sensing based approach is presented in Table 1.

3.4. Machine learning based methods

A survey on the usage of REM-based techniques for various applications of wireless regional area network has been discussed in [37]. In [37], the authors have focused on presenting the REM-enabled case and knowledge based learning

algorithms for cognitive engine based wireless regional area network as a viable solution. The detection or identification of state of PU is a key part of the REM construction. However, it is difficult to identify multiple PUs in an individual user terminal. A hidden Markov chain model has been proposed in [38] that enables the sensor nodes to identify the states of the PUs (either active or sleep) to efficiently construct the REM. An unsupervised classification method has been proposed in [39] to classify the BS–user links into two propagation models such as line-of-sight and non-line-of-sight based on their signal values. Then, maximum likelihood estimation (MLE) is used to compute the model parameters. Further, the 3D map of the area is obtained based on the category information which signifies the obstacle layout. This area map can be used to obtain the signal blockage of a corresponding BS–UE pair. Then, the signal reconstructed for that UE pair and the received signal strength (RSS) can be obtained. By considering the geographical sparsity of the power propagation map (PPM), a sparse Bayesian learning (SBL) algorithm has been proposed in [40] that can dynamically monitor the number, location, and radio power profiles of PU and base station in CR. The proposed SBL algorithm can effectively reconstruct the PPM which can be used for monitoring the spectrum usage of the PUs. The main advantage of SBL is that it only requires the SUs information such as locations, received signal strength indicator (RSSI) values, and time instants. Experimental validation of the functionality of a SC algorithm based on the adaptive RBFs has been performed in [41]. The received signal power at each location is estimated as a linear combination of different RBFs. The expectation maximization with a least squares loss function and a quadratic regularizer has been used to jointly optimize the weights of the RBFs, their Gaussian decaying parameters, and locations. In [42], the authors have used machine learning to jointly optimize the weights of the RBFs, their Gaussian decaying parameters and locations by representing the RBFs as centroids at optimal locations. Similar to [41], the expectation maximization with a least squares loss function and a quadratic regularizer has been used to jointly optimize the weights of the RBFs. In [43], the knowledge of dictionary learning and compressive sensing has been adopted to design the spectrum sensing algorithms for CRs. These algorithms can predict the interference power experienced by a CR node based on the past and current measurements made by a set of nodes. Based on the CR network topology a regularization term has been incorporated by exploiting the fact that the spatial variation of interference is smooth. Batch and online algorithms were derived, where the online alternative possessed a tracking capability at lower complexity and memory requirements. In dense urban areas, the wireless signals are blocked by building terrains. In order to address this issue, the unmanned aerial vehicles (UAVs) started being used as relays to forward the information between base station (BS) and user equipment (UE). However, the position of UAV affects the CG between BS and UE. In order to capture the signal strength and propagation conditions, the authors in [18] have exploited the finely structured radio map. However, the radio map obtained will be complex in nature due to the irregular shapes of the buildings that affect the signal strength. Thus, a machine learning approach has been proposed to reconstruct the radio map from a limited number of signal strengths obtained from a set of locations [18]. The main goal of [18] is to train a channel predictor and interpolate the CG to obtain the propagation conditions for each UAV-UE location. Then, an efficient data clustering and parameter estimation algorithm has been proposed in [8] to construct a REM between each UAV-UE pair with fine-grained propagation details by learning and reconstruction of small measurement samples. Further, a hidden multi-class virtual obstacle model has been proposed to efficiently study the air-to-ground channel. The existing SC approaches mostly depend on tomographic model, where the shadowing is modeled as the weighted integrals of spatial loss field (SLF). In general, the SLF can be learned with regularization methods depending on the propagation environment. However, the existing regularization methods are ineffective in case of heterogeneous environment. Thus, in [44], an adaptive Bayesian framework has been proposed to construct the CG maps that provide the CG between any arbitrary transmitter–receiver pairs over a heterogeneous environment. The proposed framework is based on a hidden Markov random field (MRF) model that identifies the spatial correlations of the neighboring regions exhibiting the similar statistical behavior. Further, Markov Chain Monte Carlo (MCMC) sampling has been used to derive the efficient field estimator which is a powerful tool in the absence of the analytical solutions of minimum mean square error and maximum a posteriori estimators. In order to reduce the uncertainty in the estimation of SLF, the authors have developed an adaptive data acquisition method. A detailed description on each of the compressive sensing based approach is presented in Table 2.

3.5. Other techniques

In [1], the performance comparison of three interference cartography methods namely natural-neighbor, thin-plate spline, and Kriging interpolation has been carried out for CRNs in terms of PU localization accuracy and RF field strength estimation accuracy. It has been concluded that the natural-neighbor interpolation method provides the desirable features suitable for CRNs [1]. A comparative analysis of three interpolation techniques such as Kriging, modified shepard's method, and gradient plus inverse squared method has been carried out in [45] for efficient management of spectrum resources for future wireless networks. From numerical analysis, it has been concluded that Kriging method outperforms other two in terms of relative MAE [45]. A probabilistic interference constrained method with a REM for spectrum sharing has been proposed in [46] for spatial spectrum sharing. Ordinary Kriging method has been used for the construction of REM, then, the transmit power of the PUs has been formulated based on the estimation error distribution. Subsequently, the proposed method in [46] has been compared to existing path-loss based method, the perfect estimation, and the Kriging based method without error prediction. It has been concluded that even with the small amount of measurement data, the proposed method has higher spectrum sharing opportunity in comparison to other methods. A comparative analysis of the local interpolation techniques such as nearest and natural neighbor and linear, quadratic and cubic interpolation which

Table 2
Comparison of machine learning based methods.

Method	Pros	Cons	Application/ Deployment scenario
Segmented regression approach [18]	(1) Considers segmented propagation structure of the radio map (2) Requires fewer training samples compared to KNN	Flight trajectory optimization for accelerating the learning process	UAV-aided wireless network
A comprehensive cost-efficient approach [37]	Cost efficient approach	Did not exploited the sparsity of the active users in frequency and space	(1) IEEE 802.22 Wireless regional area network (2) TV broadcast bands
Hidden Markov Model [38]	Superior to unsupervised clustering methods in the presence of both AWGN and Rayleigh fading channels	Impractical assumption that the number of primary users are known to the secondary users	Cognitive radios
Sparse Bayesian learning algorithm [40]	30% improvement in the detection of wireless microphone in comparison to existing methods	Described the distribution of power over space not over frequency	Cognitive radio systems
Adaptive RBF based SC algorithm [41,42]	(1) Does not considers the locations of sensors (2) Overcomes the limitation of multipath affect on pilot signals	Considered only Single receiver and not with multiple	Cognitive radio
Dictionary learning and compressive sensing [43]	(1) Low complexity (2) Low memory requirements	The work has mainly focused on spatial domain	Cognitive radio network

are based on Delaunay triangulation has been presented in [47] for CRNs. Primary emitter localization accuracy and RF field estimation efficiency are used as the performance metrics for evaluating the performance. Through simulations, it has been concluded that the linear interpolation technique results in the same performance as such of complex interpolation methods due to the utilization of triangulation [47]. The deployment of LTE-Advanced radio access network can improve the network capacity and data rates by utilizing licensed spectrum access (LSA) channel. LTE-Advanced networks collects each UEs' measurement data by utilizing a feature named minimization of drive test reporting system. This data provides the location and signal strength information. Motivated by this, in [48], a comparative analysis of four spatial interpolation techniques such as Nearest Neighbor (NN), inverse distance weighting, triangular irregular network, and Kriging has been presented for LTE-Advanced networks to estimate the interference map and the effect of spatial correlation and errors in the measurement estimation has been studied.

In [49], the advantage of directional antenna has been considered in order to estimate the unknown locations and transmit powers of PUs. The area of interest, where the PUs are present, is divided into M grid points and it has been assumed that the PUs may present within each grid. A set of sensor nodes with an antenna, each with elements of uniform linear array, have been deployed to track the PUs. Then, the locations and powers of PUs have been modeled by a sparse vector in which the elements are non-zero in the presence of a PU in the corresponding grid. Moreover, centralized and distributed source localization algorithms have been developed in which the received signal strength (RSS) and direction of arrival (DoA) are unified as a single field. In the centralized setup, a compressive sensing problem has been established at fusion center. In the distributed setup, each sensor node shares the collected information with the neighbors and then, each SU applies compressive sensing algorithm based on the information collected from neighboring SUs. It has been shown that the proposed framework is applicable for dynamic SC [49]. A novel Kriged Kalman filtering (KKF)-based algorithm has been proposed in [50] that can capture optimal estimates of the unknown CGs of arbitrary locations for a given area using measurements corresponding to CRs. This algorithm adopted the dynamic shadow fading that can capture both spatial and temporal correlations. A distributed version of the KKF algorithm, derived using alternating direction method of multipliers, requires just local message passing yet construct the global view of the CG maps through concurrent iterations. A Shepard's interpolation technique has been considered in [51] to construct a spectrum map by fusing the information shared by SUs with a consideration of their mutual distances and spatial orientation with each other. Then a vector clustering technique that uses the tree structured vector quantization has been developed to determine the optimal locations of the SUs [51]. In [52], a REM is constructed by utilizing the interference cartography and geo-graphical locations of the users for CR based heterogeneous networks. The extraction of geo-locations of users gives a viable picture of the environment for efficient detection, analysis, and decision. The advances in signal processing techniques are utilized to extract the geo-locations of users efficiently. It has been shown that the proposed mechanism allows the SUs to efficiently access the licensed band without creating interference to the PUs [52]. In [53], the need for REM dissemination for CR networks has been discussed in order to reduce the network overhead. Then, the performance comparison of different REM dissemination techniques under various network scenarios has been carried out. Finally, the authors have discussed the ways to enhance the efficiency of REM dissemination and claimed that the REM dissemination can be significantly reduced by extending the optimized link state routing protocol [53]. In [54], cooperative CR sensing problem has been considered and novel spectrum sensing algorithms have been proposed to track the CG maps of PUs present in a given

geographical area. Here, CG maps capture the propagation characteristics per frequency from any geographical location to a CR user. Further, the Kriged Kalmann filtering has been considered to update the CG maps in real time. Then, a sparse regression technique has been considered to track the transmit power and locations of unknown PUs in that area.

Two indirect methods to construct the REM have been proposed in [55]. The first one is based on the received signal strength difference (RSSD) and second is based on RSS. These two indirect methods are compared using log-normal shadowing under different scenarios. These scenarios include different number of sensor nodes, several shadowing spread values, mobility of the sensor nodes. Through results, the authors claimed that the number of sensor nodes and number of measurements considered has more effect on the REM [55]. In [16], it has been shown that the sensor measurements convey more information than spatial loss fields in existing methods. In existing approaches the sensor measurement conveys spatial loss field whereas the weights of the SLF is selected heuristically whose effectiveness is not clear. Motivated by this, in [16], a blind channel gain cartography method has been proposed that extract both SLF and the corresponding weights to obtain the CG maps of the area of interest. A low rank plus sparse matrix model has been proposed in [56] for CG cartography. In this work, the CGs have been modeled as the tomographic accumulations of SLF that capture the pathloss model of the channel. Here, the SLF was assumed to have a low-rank structure corrupted by sparse outliers. Then, the authors have derived efficient batch and online algorithms by leveraging a bifactor-based characterization of the matrix nuclear norm. In [57], it has been mentioned that the existing SC methods construct the power maps from power measurements and PSD maps from PSD measurements by leveraging the framework of kernel-based learning. In contrast to the existing methods, in [57], the authors have presented a family of methods for nonparametric and semiparametric estimation of the PSD maps from RF power measurements. The proposed methods support the low-cost and low-power sensor nodes as it is the estimation of RF power distribution over frequency and space. In [58], a joint indoor localization and radio map construction method has been proposed for indoor environment that can be employed with limited number of calibration fingerprints and source data set preserving spatial correlation. The proposed method transfers the knowledge of this data set to calibration fingerprints and localization observations to perform localization directly without radio map using manifold alignment. The method in [58] can also construct the radio map by accumulating history of localized readings. In [59], the authors have divided the area of interest into clusters and in each cluster a group of sensor nodes are deployed to collect the temporal correlation for a particular cluster, not over the entire area and the Nyquist rate differs from group to group. Then, a fusion center collects these groups of temporal correlation estimates and process all with the combined Nyquist rate to estimate the PSD of over entire area. The main advantage of the proposed mechanism is that the required sampling rate for each sensor node is less compare to the no cluster based approach. In [60], the authors have proposed a REM construction technique that is based on active transmitter location estimation. Further, in [60], the authors have claimed that the proposed active transmitter location estimation based REM construction mechanism outperforms the existing mechanisms such as Kriging and inverse distance weighted interpolation methods in multipath and shadow fading channels in terms of RMSE. In [61], a novel spectrum sensing based REM construction method has been proposed that forms a single heterogeneous testbed by integrating both mid-end and low-end spectrum sensing devices. The performance of the proposed integrated system in [61] has been analyzed in terms of accuracy of REM construction in real-time. In [62], the authors have considered the application of spatial ordinary Kriging (OK) interpolation method for platoon based cellular vehicle to anything (V2X) communication. With an assumption of availability of geo-localized received power values, OK interpolation method is used to reconstruct the REM by estimating at other platoon vehicle locations. Through extensive numerical results, it has been concluded that the OK is able to reconstruct the REM with acceptable MSE and also reduces the control information for REM acquisition up to 64% [62]. A distributed incremental clustering (DIC) algorithm has been proposed in [63] for future 5G automotive to reduce the number of sensor nodes required for the construction of REM. The DIC algorithm based on regression Kriging (RK) method can efficiently estimate the average received power at locations where the sensor nodes are absent. Through extensive results, the authors have claimed that path-loss and shadowing components are important for efficient channel map construction. Further, the authors have claimed that the RK method leads to superior performance in comparison to ordinary Kriging method [63]. In [64], the authors have proposed basic method for the construction interference cartography for licensed networks in order to mitigate the interference caused by an license shared access-licensed LTE-advanced Radio Access Network (RAN) in the uplink. The performance of the proposed method is compared with the spatial interpolation techniques such as nearest neighbor, inverse distance weighing (IDW), and Kriging method. It has been concluded that basic method outperforms the interpolation techniques in terms of correct rejections and false alarms, however, the interpolation techniques dominates in terms of hit and miss percentage. Further, it has been noticed that Kriging interpolation method outperforms all in overall [64]. In [65], the authors have aimed at constructing the REM using energy detector for the coexistence of the terrestrial and satellite networks. This allows the satellite users to access the resources unused by the terrestrial networks. In [66], the authors have used Discrete Cosine Transform (DCT) for constructing the radio frequency map and a simulation study has been presented to compare the performance of DCT with the other interpolation techniques. It has been claimed that DCT is more dynamic and accurate technique in comparison to IDW method. In [67], a linear tomographic method has been used to construct the radio map in order to obtain the shadowing attenuation between any two given points in the map. Here, the authors have considered the shadowing attenuation as the weighted integral of spatial loss field. The proposed algorithm finds the solution in an iterative way by relying on the alternating direction method of multipliers [67]. In [68], the authors have discussed the ways to construct REM for TV signals in the context of indoor and outdoor environments using ordinary Kriging algorithm.

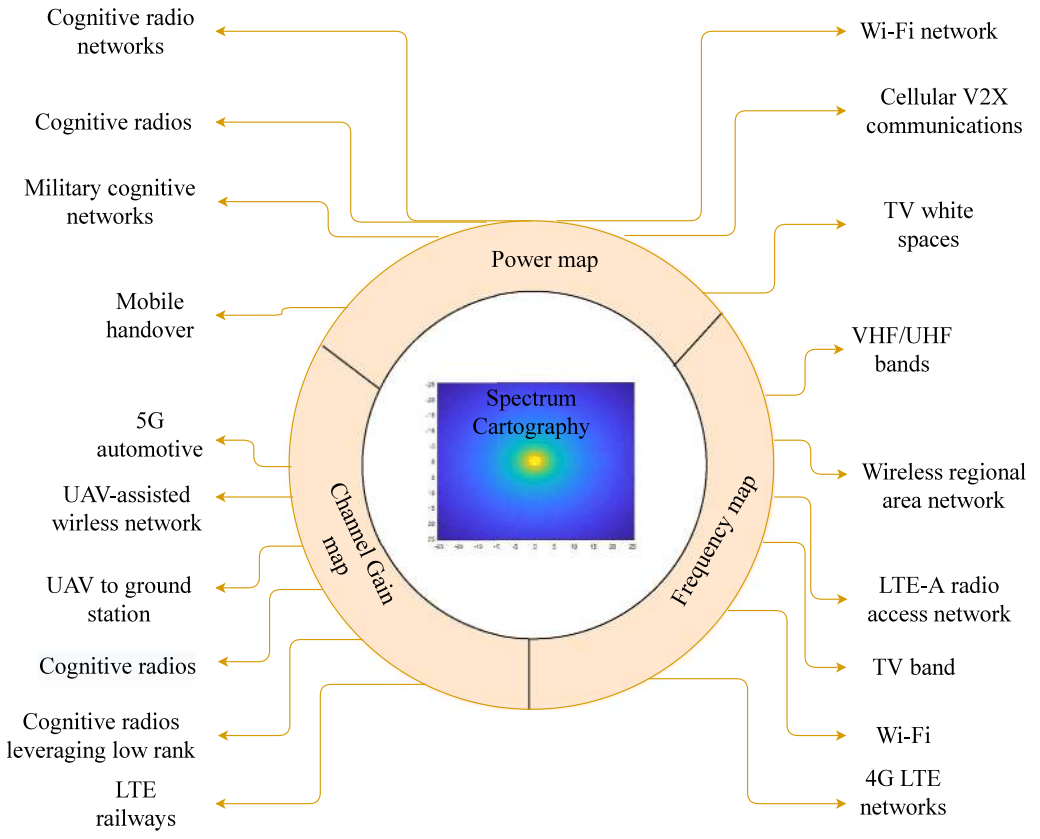

Fig. 2. Applications of Spectrum Cartography.

Then, they have used multiple methods to construct the REM from real time data collected from Poznan and Poland. Finally, the authors have discussed the new approaches to consider the attenuation from walls while constructing the REM [68]. In [69], the authors have proposed a framework to construct the 3D spectrum map based on region of interest (ROI)-driven UAV deployment for efficient spectrum construction and management in smart IoT. The proposed framework in [69] is composed of four stages such as pre-sampling, spectrum situation estimation, ROI-driven UAV deployment, and total variance based spectrum map reconstruction.

3.6. Open challenges and future scope

The UAVs have gained significant attention in many applications as they can be used as flying relays for wireless networks. The dynamic change in network topology has lead to many spectrum mapping and communication challenges. One such challenge is the construction of 3D REM that includes both space and time. The state-of-the-art SC mechanisms focused on the construction of 2D REM, however, very limited research has been done for the construction of 3D REM [69]. The 3D data to be collected and processed is huge. Thus, future works should focus on the compressive sensing based 3D REM construction approaches that require less data to process to accurately construct the REM. Further, machine learning based approaches are more suitable to learn the dynamic change in the network topology to efficiently construct REM. The novel approaches that include both compressive sensing and ML seem to be more efficient as they can track the dynamic network topology and construct the REM with limited data and processing time.

3.7. Applications of REM

- In [70], the authors have proposed a spectrum sharing technique for CRNs that allows the SUs to share the spectrum with the PUs by exploiting REM. Further, the authors have developed REM-enabled CR adaptation algorithms for both open area and dense urban area. A simulation analysis has been presented to compare the performance of global REM and local REM. It has been claimed that the CR can make situation-aware adaptations in topology, routing protocols, transmit power, and transmission timing leading to reduced interference to PUs. Further, the global REM method has been used to mitigate the problem of hidden node or hidden receiver.

- A framework for REM-enabled situation aware learning algorithm has been proposed in [71], that allows the SUs to coexist with the PUs without causing more interference. Further, it has shown that the proposed mechanism in [71] mitigates the hidden node problem.
- A REM enabled soft frequency reuse scheme has been proposed in [72] to improve the throughput of the 4G LTE networks by 14%. In [72], the REM stores signal strength and traffic maps and then, the BSs' subchannel transmit powers tuned so as to maximize the throughput.
- In [9], the authors have proposed the REM enabled scheme for controlling the transmit power levels of base stations in 4G/5G networks without causing the interference to licensed band. This enables the dynamic spectrum access so as to increase the network throughput in both indoor and outdoor networks.
- Local cartography-based dynamic spectrum access technique has been proposed in [73] that allocates the joint power and frequency resource blocks (RBs) by creating the interference map. In this mechanism, the SUs classify resource blocks at target locations and use them for transmission with required power levels without disturbing the PUs which enhance the throughput.
- In [10], cognitive Doppler spread compensation (CDSC) algorithms have been proposed for HSTs that compensate the time-varying Doppler spread by using the REM. Here, REM contains the spatial–temporal information of the radio channel parameters along a given railway. It has been claimed that the proposed CDSC algorithm is more efficient in comparison to the typical OFDM based broadband mobile system which presents a new paradigm for mobile communication in HSPs.
- The estimation of Doppler shift for HSTs is a big challenge. Motivated by this, in [74], a Doppler shift estimation algorithm has been proposed for an OFDM based HSTs. The REM has been constructed which includes Doppler shift information, from the field tests by using the HST time tables, regular and repetition routes. Then, maximum a posteriori estimator (MAPE) has been proposed to estimate the Doppler shift accurately. MAPE exploits the cyclic prefix structure for OFDM using REM and obtains the MAP estimates. It has been claimed that the proposed mechanism outperforms REME and classical CP based estimator in terms of mean square error (MSE) [74].
- A user handover algorithm based on the REM has been proposed in [75] that predicts the best network connection based on the constructed REM. Through extensive Monte Carlo simulations it has been claimed that a 10% reduced in the ping pong handovers can be achieved with the proposed handover algorithm [75].
- An emulation based analysis has been carried out in [76] in three cities of Japan to help the SUs to find the free band in TV white spaces. Fig. 2 provides an overview of all the applications of spectrum cartography.

4. Performance analysis

In this section, we provide the simulation results for the comparison of the actual REM and reconstructed REM with NN method [1] that is used frequently in the literature. We consider a grid of 25×25 with the locations of PUs at grid points. Then, 50 sensor nodes randomly deployed in the grid to extract the data. We consider the unit distance $d_0 = 1$ m, the reference power at unit distance is 20 dBm, and the path-loss exponent (α) is, 2 [77], for the calculation of received power and CG towards power map and CG map, respectively. We consider $\beta = -30$, $\alpha = 3.64$, $\sigma^2 = 3$, $c = 3 \times 10^8$ m/s, and $f = 1080$ MHz for the calculation of received power for frequency map.

Figs. 3 and 4 show the image and surface plots of the actual and reconstruction maps, respectively, with a single REM-acquisition unit (REM-AU) at the center of the grid. Figs. 3(a) and 4(a) show the image plot and surface plots, respectively, of actual power map at the exact locations of the primary devices. We consider the REM-AU at the center of the grid and the received signal strength is calculated from (1). From Figs. 3(a) and 4(a), it is observed that the received signal strength is high at the grid points near the REM-AU as the distance is less. However, when we go from away from the center, the RSSI reduces in a logarithmic manner due to the attenuation. Figs. 3(b) and 4(b) show the image and surface plot of the reconstructed map with NN method considered with 400 sensor nodes deployed randomly in the grid. From Figs. 3(b) and 4(b), it is observed that the reconstructed power map is similar to the actual map. However, it is not same with the actual map as the NN method chooses the NN to estimate the RSSI at a particular grid location. Figs. 3(c) and 4(c) show the image and surface plot of the CG map constructed from (2). Since the CG also depends on the distance of the user from the REM-AU, the CG values are more for the locations near the REM-AU. The peak values near the center in Fig. 4(c) represents the same. However, when the devices are away from the REM-AU, the CG values decreases. Additionally, the blue color in Fig. 3(c) represents the same. Figs. 3(d) and 4(d) show the image and surface plot of the reconstructed CG map with NN method considered with 400 sensor nodes deployed in the grid. From Figs. 3(d) and 4(d), it is observed that the reconstructed CG map is similar to the actual map. However, it is not same as the actual map, because the NN method chooses the NN to estimate the CG at a particular grid location. Figs. 3(e) and 4(e) show the image and surface plot of the frequency map constructed from (3). From (3), it is noted that the RSSI is a function of both frequency and distance. However, in this work, we consider a constant frequency of 1080 MHz, hence, the RSSI also depends on the distance. Thus, the RSSI values are high at the grid points near the REM-AU which can be observed from the peak at the center in Fig. 4(e). Figs. 3(f) and 4(f) illustrate the image and surface plot of the reconstructed frequency map with NN method considered with 400 sensor nodes deployed over the grid. From Figs. 3(f) and 4(f), it is observed that the reconstructed frequency map is almost matches with the actual map as the RSSI depends on the frequency and we consider fixed frequency herein.

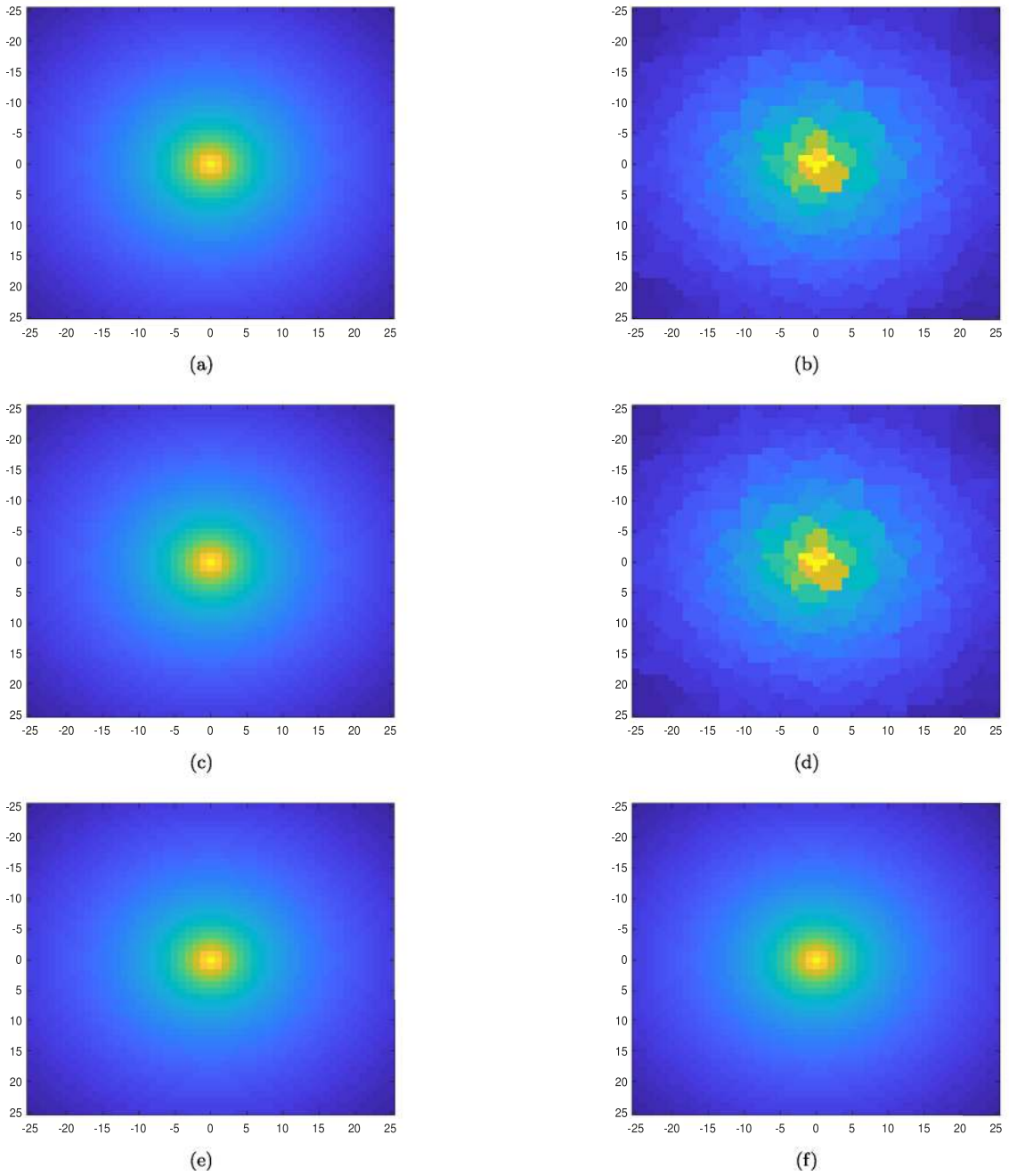

Fig. 3. An illustration of (a) Actual power map and (b) Reconstructed power map (c) Actual CG map (d) Reconstructed CG map (e) Actual Frequency map and (f) Reconstructed Frequency map using NN method with 400 sensor nodes deployed in the grid.

Figs. 5(a), 5(b), 5(c), and 5(d) depict the variation of MAE, MSE, NMSE, and RMSE with increasing number of sensor nodes for single REM-AU. Here, we varied the number of sensor nodes from 50 to 750. From Fig. 5, it is observed that all the errors are more for CG maps in comparison to other maps. CG values decreases 36.4 times the logarithmic of distance for CG map whereas for other maps the RSS decreases 20 times the logarithmic of distance. Further, it is observed that the error decreases with increasing number of sensor nodes as the number of sensor nodes near the grid locations increases.

Figs. 6 and 7 show the image and surface plots of the actual and reconstructed maps with respect to all three maps, respectively, consisting three REM-AUs at $(-10, -10)$, $(0, 0)$, and $(13, 13)$. From Figs. 6 and 7, it is observed that the reconstructed map is almost similar to the actual map for all three maps even though there is a difference in the peak

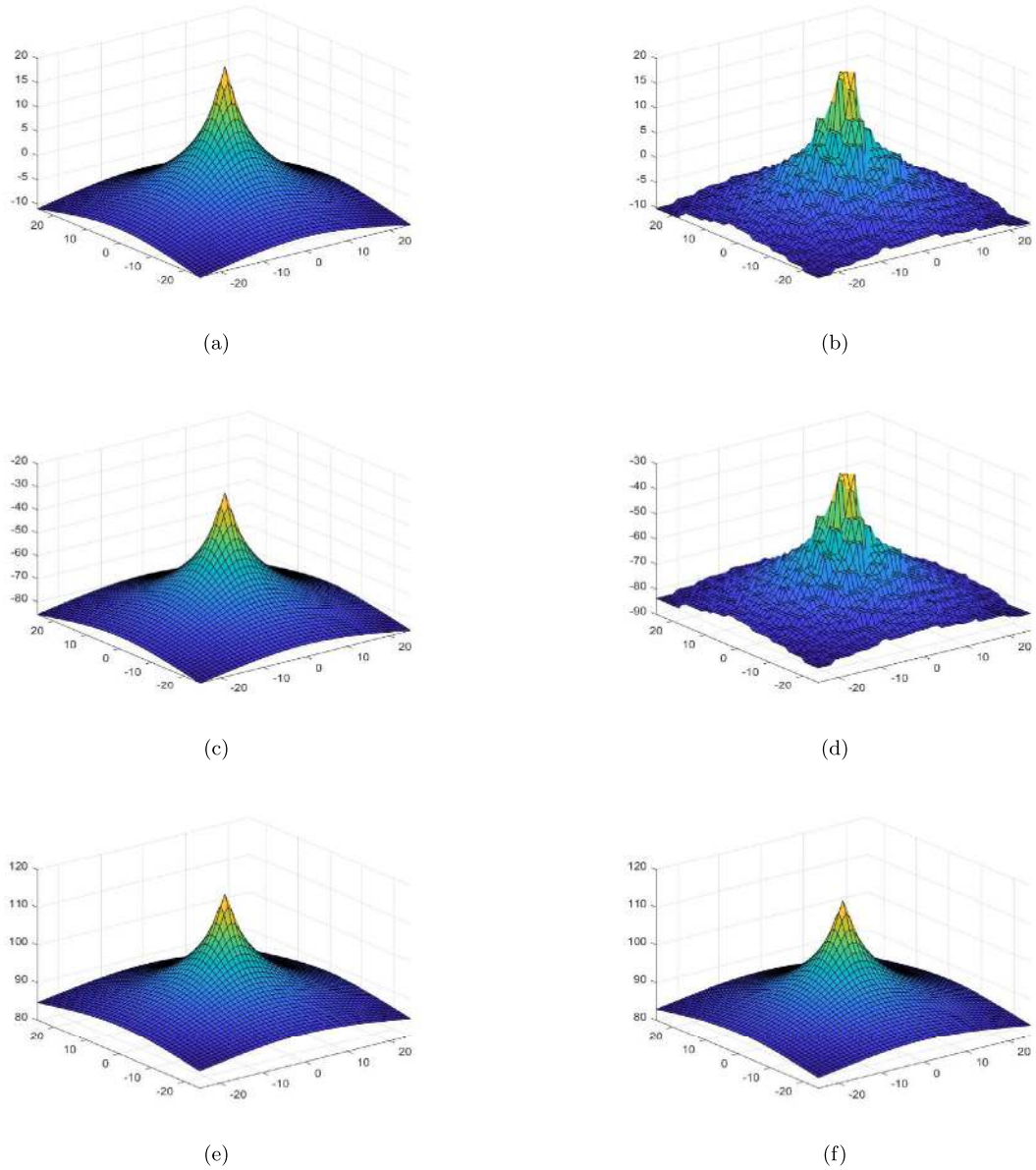

Fig. 4. An illustration of (a) Actual power map and (b) Reconstructed power map (c) Actual CG map (d) Reconstructed CG map (e) Actual Frequency map and (f) Reconstructed Frequency map using NN method with 400 sensor nodes deployed in the grid.

values which is not the case for single REM-AU as can be observed from Figs. 3 and 4. This is due to the fact that a sensor node reports to the REM-AU which is near to it. Since the distance from NN of a location to the REM-AU is less, the error is less.

Figs. 8(a), 8(b), 8(c), and 8(d) illustrate the variation of MAE, MSE, NMSE, and RMSE with increasing the number of sensor nodes with three REM-AUs. Similar to single REM-AU case considered in Fig. 5, we varied the number of sensor nodes from 50 to 750. From Fig. 8, it is observed that all the errors are more for CG maps in comparison to other maps. Further, the error values are less for three REM-AU case in comparison to single REM-AU case as the NN method almost recreates the map. Moreover, it is observed that the error decreases with increasing number of sensor nodes as the number of sensor nodes near the grid locations increases.

Finally, Tables 3–5 demonstrate the summary of performance comparison of the recent SC methods proposed for the construction of power map, CG map, and frequency map, respectively. It is observed from Table 4 that, adaptive Bayesian framework results in the improved performance for the construction of CG map as it requires only 30% less number of samples for the construction of map as compared to other methods. It is also observed from Table 5 that an efficient

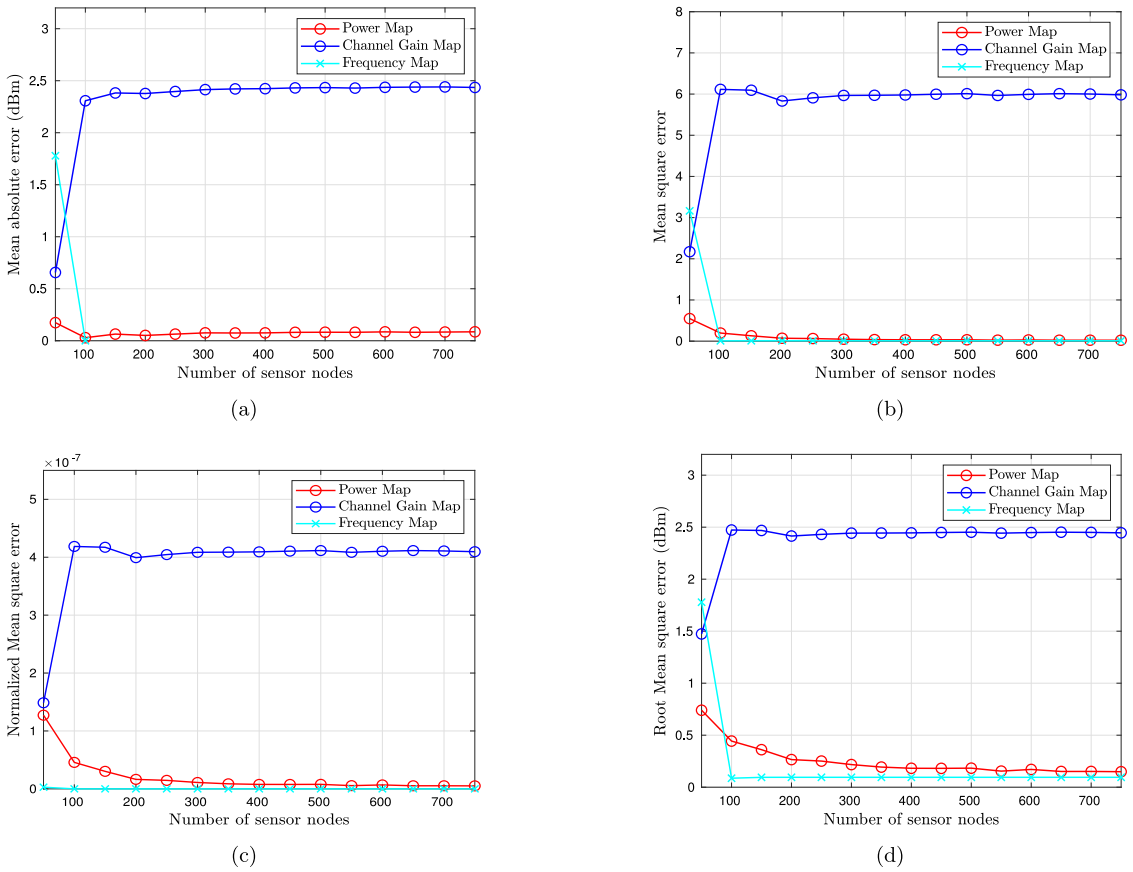

Fig. 5. Variation of (a) MAE, (b) MSE, (c) NMSE, and (d) RMSE with increasing number of sensor nodes for the reconstruction of power map, CG map, and frequency map using NN method.

Table 3
The state-of-the-art for power maps.

Method	Map considered	Kind of study	Parameters
SC algorithm in [30]	PSD map	Simulation	MSE
Location free SC method [33]	Power maps	Simulation	NMSE
Coupled block-term tensor decomposition framework [34]	Power map	Simulation	Normalized absolute error
Non-parametric SC algorithm [35]	PSD map	Simulation	NMSE
Online SC method [36]	PSD map	Simulation	Efficiency
SBL algorithm [40]	Power propagation map	Simulation	Normalized RMSE
SC method based on adaptive RBFs [41]	PSD maps	Experimental	NMSE
Machine learning for adaptive RBFs [42]	PSD maps	Experimental	NMSE
Usage of directional antenna [49]	Power maps	Experimental	MSE, Normalized error
Two indirect methods [55]	REM	Simulation	Transmitter location error
Nonparametric and semiparametric methods [57]	PSD maps	Simulation	NMSE
Distributed incremental clustering (DIC) algorithm [63]	Power maps	Simulation	MSE

data clustering and parameter estimation algorithm reduces the radio frequency REM reconstruction time by 300% when compared to conventional methods. Further, machine learning based approaches have increased the MSE for radio map reconstruction by 90%.

Table 6 illustrates the complexity analysis of some of the state-of-the-art SC methods. Here, M and N represent the number of estimating REM locations and measurements with $M, N \rightarrow \infty$, $M > N$. P and p denote the order of the spline function and number of unknowns in linear system of equations.

5. Conclusion

In this paper, we have presented the state-of-the-art on the spectrum cartography (SC) techniques available for the construction of radio environment map (REM). We have discussed the architecture of SC and presented the expressions

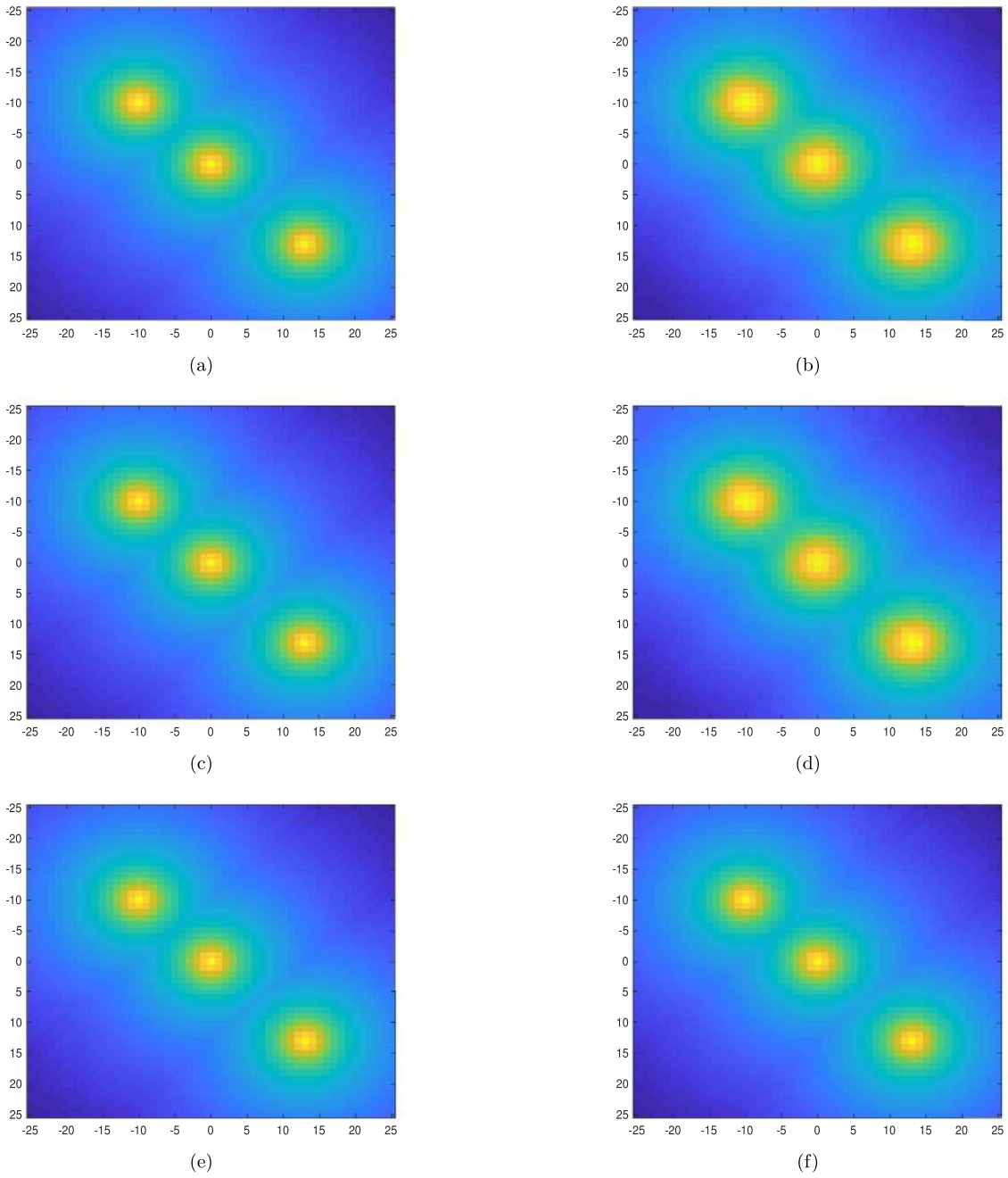

Fig. 6. An illustration of (a) Actual power map and (b) Reconstructed power map (c) Actual CG map (d) Reconstructed CG map (e) Actual Frequency map and (f) Reconstructed Frequency map using NN method with 400 sensor nodes deployed in the grid.

Table 4
The state-of-the-art for CG maps.

Method	Map considered	Kind of study	Parameters
Adaptive Bayesian framework [44]	CG maps	Experimental	SLF
Kriged Kalmann filtering-based algorithm [50]	CG map	Simulation	RMSE
Cooperative CR sensing [54]	CG maps	Simulation	MSE
A low rank sparse matrix model [56]	CG map	Experimental	NMSE

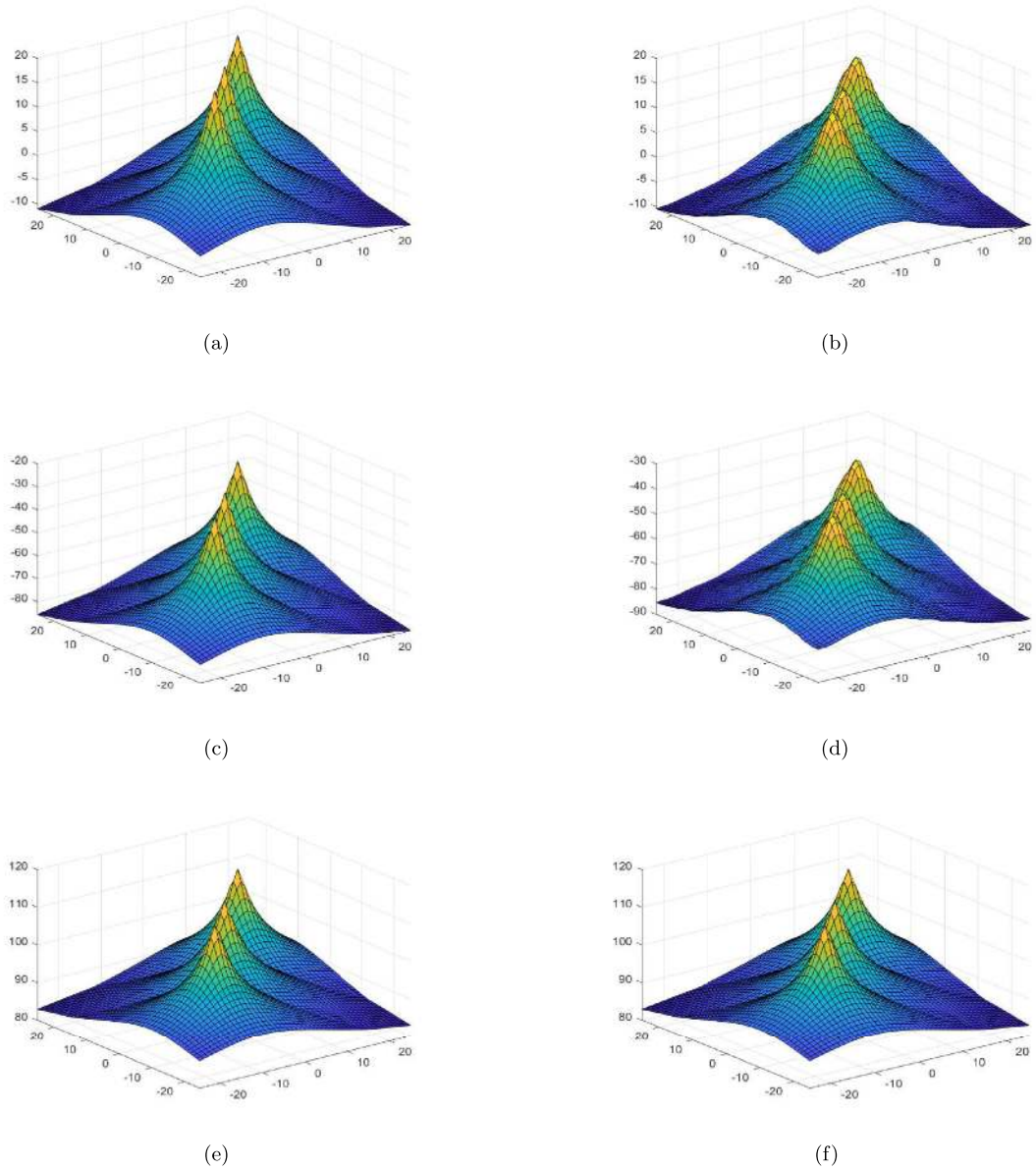

Fig. 7. An illustration of (a) Actual power map and (b) Reconstructed power map (c) Actual CG map (d) Reconstructed CG map (e) Actual Frequency map and (f) Reconstructed Frequency map using NN method with 400 sensor nodes deployed in the grid.

for received signal strength for power and frequency map and channel gain (CG) for CG map. We have discussed the REM construction methods based on compressive sensing, which use less sensor data to construct REM. Subsequently, we discussed machine learning based approaches, which are mostly learning based approaches for dynamic spectrum access. Through extensive simulations, we have presented the various REMs and surface plots corresponding to the actual maps and reconstructed maps with NN method to provide an overview of REM construction and evaluated the performance of nearest neighbor (NN) with MAE, MSE, NMSE, and RMSE. Finally, we have tabulated the summary of various state-of-the-art mechanisms for constructing REMs. It has been observed that adaptive Bayesian framework results in the improved performance for the construction of CG map as it requires only 30% less number of samples for the construction of map as compared to other methods. An efficient data clustering and parameter estimation algorithm reduces the radio frequency REM reconstruction time by 300% when compared to conventional methods. Further, machine learning based approaches have increased the MSE for radio map reconstruction by 90%.

The state-of-the-art SC mechanisms focused on the construction of 2D REM, however, very limited research has been done for the construction of 3D REM. Thus, future works should focus on the compressive sensing based 3D REM

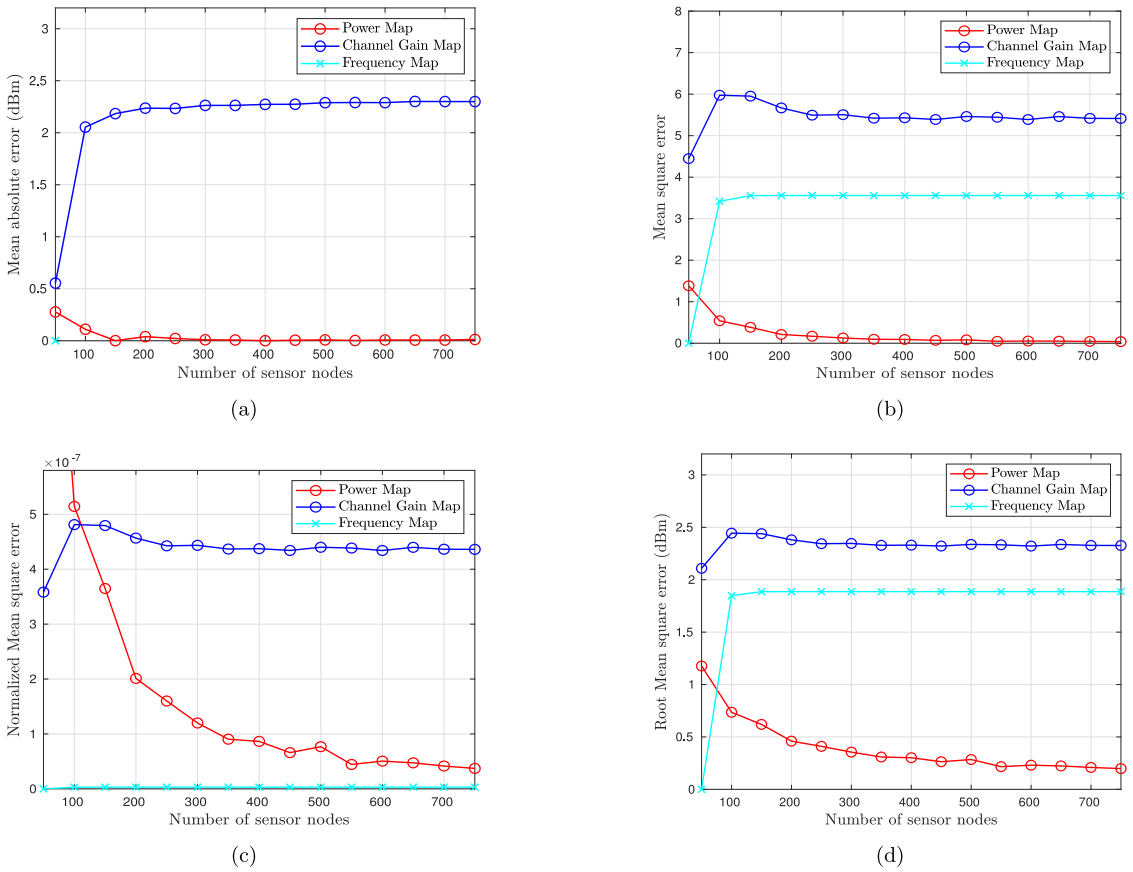

Fig. 8. Variation of (a) MAE, (b) MSE, (c) NMSE, and (d) RMSE with increasing number of sensor nodes for the reconstruction of power map, CG map, and frequency map with NN method in the presence of three REM-AUs.

Table 5
The state-of-the-art for frequency maps.

Method	Map considered	Kind of study	Parameters
Data clustering and parameter estimation algorithm [8]	Radio map	Simulation	REM reconstruction time
ML approach [18]	Radio map	Simulation	MSE
CSMC [29]	Interference map	Experimental	Number of samples
Compressive sensing problem [31]	Frequency map	Simulation	Reconstruction error
Compressive sensing based approach [32]	Frequency map	Simulation	Probability of false alarm Standard deviation 0.95 probability of cutoff
Sparse Bayesian learning algorithm [40]	REM map	Simulation	RSME, MSE
Kriging, modified shepard's method, and gradient plus inverse squared method [45]	REM map	Simulation	RMAE
Nearest and natural neighbor and linear, quadratic and cubic interpolation based on Delaunay triangulation [47]	Interference map	Simulation	RMSE, Efficiency
Spatial interpolation techniques such as Nearest Neighbor (NN), inverse distance weighting, triangular irregular network, and Kriging [48]	Interference map	Simulation	RMSE
DCT [66]	Interference map	Simulation	RMSE, efficiency
3D spectrum map framework [69]	Frequency map	Simulation	RMSE
Doppler shift estimation algorithm [74]	Frequency map	Simulation	MSE

construction approaches that require less data to process to accurately construct the REM. Further, machine learning based approaches are more suitable to learn the dynamics in the network topology to efficiently construct REM. Finally,

Table 6
Complexity analysis.

Method	Complexity
Inverse distance weighted interpolation method [78–80]	$O(MN)$
Nearest neighbor method [81,82]	$O(M \log N)$
Spline method [83]	$O(MNP^2)$
Natural neighbor method [78,81]	$O(M(N+k)\log N)$
Modified Shepard's method [78,84]	$O(M \log N)$
Gradient plus inverse distance squared method [85]	$O(M \log N)$
Ordinary Kriging method [86]	$O(MN^2)$
LIvE method [87]	$O(MN^{2.376})$
SNR-aided method [88]	$O(Np^2)$
Indirect indoor method [89]	$O(Np^2)$

we claim that novel approaches that includes both compressive sensing and ML are more efficient as they can track the dynamic network topology and construct the REM with limited data.

Declaration of competing interest

The authors declare that they have no known competing financial interests or personal relationships that could have appeared to influence the work reported in this paper.

Acknowledgments

This work was supported by the Indo-Norwegian Collaboration in Autonomous Cyber–Physical Systems (INCAPS) project: 287918 of the INTPART program and the Low-Altitude UAV Communication and Tracking (LUCAT) project: 280835 of the IKTPLUSS program from the Research Council of Norway.

References

[1] S. Üreten, A. Yongaçoğlu, E. Petriu, A comparison of interference cartography generation techniques in cognitive radio networks, in: 2012 IEEE International Conference on Communications, ICC, 2012, pp. 1879–1883, http://dx.doi.org/10.1109/ICC.2012.6364111.
[2] A.B.H. Alaya-Feki, S.B. Jemaa, B. Sayrac, P. Houze, E. Moulines, Informed spectrum usage in cognitive radio networks: Interference cartography, in: 2008 IEEE 19th International Symposium on Personal, Indoor and Mobile Radio Communications, 2008, pp. 1–5, http://dx.doi.org/10.1109/PIMRC.2008.4699911.
[3] J.A. Bazerque, G.B. Giannakis, Distributed spectrum sensing for cognitive radio networks by exploiting sparsity, IEEE Trans. Signal Process. 58 (3) (2010) 1847–1862, http://dx.doi.org/10.1109/TSP.2009.2038417.
[4] S. Haykin, Cognitive radio: brain-empowered wireless communications, IEEE J. Sel. Areas Commun. 23 (2) (2005) 201–220, http://dx.doi.org/10.1109/JSAC.2004.839380.
[5] Q. Zhao, A. Swami, A survey of dynamic spectrum access: Signal processing and networking perspectives, in: 2007 IEEE International Conference on Acoustics, Speech and Signal Processing - ICASSP '07, Vol. 4, 2007, http://dx.doi.org/10.1109/ICASSP.2007.367328, IV-1349-IV-1352.
[6] Q. Zhao, B.M. Sadler, A survey of dynamic spectrum access, IEEE Signal Process. Mag. 24 (3) (2007) 79–89, http://dx.doi.org/10.1109/MSP.2007.361604.
[7] S. Subramani, et al., Towards practical rem-based radio resource management, in: 2011 Future Network Mobile Summit, 2011, pp. 1–8.
[8] J. Chen, O. Esrafilian, D. Gesbert, U. Mitra, Efficient algorithms for air-to-ground channel reconstruction in uav-aided communications, in: 2017 IEEE Globecom Workshops, GC Wkshps, 2017, pp. 1–6, http://dx.doi.org/10.1109/GLOCOMW.2017.8269065.
[9] Paweł Kryszkiewicz, Adrian Kliks, Łukasz Kułacz, Hanna Bogucka, George P. Koudouridis, Marcin Dryjański, Context-based spectrum sharing in 5 g wireless networks based on radio environment maps, Wirel. Commun. Mob. Comput. (2018) http://dx.doi.org/10.1155/2018/3217315.
[10] J. Li, Y. Zhao, Radio environment map-based cognitive doppler spread compensation algorithms for high-speed rail broadband mobile communications, EURASIP J. Wireless Commun. Networking (1) (2012) 263, http://dx.doi.org/10.1186/1687-1499-2012-263.
[11] H.B. Yilmaz, T. Tugcu, F. Alagöz, S. Bayhan, Radio environment map as enabler for practical cognitive radio networks, IEEE Commun. Mag. 51 (12) (2013) 162–169, http://dx.doi.org/10.1109/MCOM.2013.6685772.
[12] J. Perez-Romero, et al., On the use of radio environment maps for interference management in heterogeneous networks, IEEE Commun. Mag. 53 (8) (2015) 184–191, http://dx.doi.org/10.1109/MCOM.2015.7180526.
[13] J. Van De Beek, et al., How a layered rem architecture brings cognition to today's mobile networks, IEEE Wirel. Commun. 19 (4) (2012) 17–24, http://dx.doi.org/10.1109/MWC.2012.6272419.
[14] Tao. Cai, et al., Design of layered radio environment maps for ran optimization in heterogeneous lte systems, in: 2011 IEEE 22nd International Symposium on Personal, Indoor and Mobile Radio Communications, 2011, pp. 172–176, http://dx.doi.org/10.1109/PIMRC.2011.6139803.
[15] I. Kakalou, K. Psannis, S.K. Goudos, T.V. Yioultsis, N.V. Kantartzis, Y. Ishibashi, Radio environment maps for 5 g cognitive radio network, in: 2019 8th International Conference on Modern Circuits and Systems Technologies, MOCAST, 2019, pp. 1–4, http://dx.doi.org/10.1109/MOCAST.2019.8741554.
[16] D. Romero, D. Lee, G.B. Giannakis, Blind channel gain cartography, in: 2016 IEEE Global Conference on Signal and Information Processing, GlobalSIP, 2016, pp. 1110–1115, http://dx.doi.org/10.1109/GlobalSIP.2016.7906014.
[17] M. Lee, D. Han, Voronoi tessellation based interpolation method for wi-fi radio map construction, IEEE Commun. Lett. 16 (3) (2012) 404–407, http://dx.doi.org/10.1109/LCOMM.2012.020212.111992.
[18] J. Chen, U. Yatnalli, D. Gesbert, Learning radio maps for uav-aided wireless networks: A segmented regression approach, in: 2017 IEEE International Conference on Communications, ICC, 2017, pp. 1–6, http://dx.doi.org/10.1109/ICC.2017.7997333.

[19] Roberto Calvo-Palomino, Héctor Cordobés, Markus Engel, Markus Fuchs, Pratiksha Jain, Marc Liechti, Sreeraj Rajendran, Matthias Schäfer, Bertold Van den Bergh, Sofie Pollin, Domenico Giustiniano, Vincent Lenders, Electrosense+: Crowdsourcing radio spectrum decoding using IoT receivers, Comput. Netw. 174 (2020) 107231, http://dx.doi.org/10.1016/j.comnet.2020.107231.
[20] G. Baruffa, M. Femminella, M. Pergolesi, G. Reali, Comparison of mongodb and cassandra databases for spectrum monitoring as-a-service, IEEE Trans. Netw. Serv. Manag. 17 (1) (2020) 346–360, http://dx.doi.org/10.1109/TNSM.2019.2942475.
[21] Martian, Real-time spectrum sensing using software defined radio platforms, Telecommun. Syst. 64 (4) (2017) 749–761, http://dx.doi.org/10.1007/s11235-016-0205.
[22] M. Suchański, P. Kaniewski, J. Romanik, E. Golan, Radio environment map to support frequency allocation in military communications systems, in: 2018 Baltic URSI Symposium, URSI, 2018, pp. 230–233, http://dx.doi.org/10.23919/URSI.2018.8406717.
[23] M. Suchanski, P. Kaniewski, J. Romanik, E. Golan, K. Zubel, Radio environment maps for military cognitive networks: Deployment of sensors vs. map quality, in: 2019 International Conference on Military Communications and Information Systems, ICMCIS, 2019, pp. 1–6, http://dx.doi.org/10.1109/ICMCIS.2019.8842720.
[24] K. Zubel, J. Romanik, E. Golan, K. Wilgucki, Measurement method for construction of the radio environment maps supporting cognitive radios, in: J. Matuszewski P. Kaniewski (Ed.), Radioelectronic Systems Conference 2019, International Society for Optics and Photonics, SPIE, 2020, pp. 517–531, http://dx.doi.org/10.1117/12.2565224, 11442.
[25] P.N. Karthik, R. Ramakrishna, G. Joseph, C.R. Murthy, J. Sebastian, N.B. Mehta, Modelbased interference cartography and visualization, in: 2016 Twenty Second National Conference on Communication, NCC, 2016, p. 1, http://dx.doi.org/10.1109/NCC.2016.7561174.
[26] V. Chowdappa, C. Botella, B. Beferull-Lozano, Distributed clustering algorithm for spatial field reconstruction in wireless sensor networks, in: 2015 IEEE 81st Vehicular Technology Conference, VTC Spring, 2015, p. 1, http://dx.doi.org/10.1109/VTCSpring.2015.7145783.
[27] F. Frantzis, V. Chowdappa, C. Botella, J.J. Samper, R.J. Martinez, Radio environment map estimation based on communication cost modeling for heterogeneous networks, in: 2017 IEEE 85th Vehicular Technology Conference, VTC Spring, 2017, p. 1, http://dx.doi.org/10.1109/VTCSpring.2017.8108227.
[28] G. Boccolini, G. Hernández-Peñaloza, B. Beferull-Lozano, Wireless sensor network for spectrum cartography based on kriging interpolation, in: 2012 IEEE 23rd International Symposium on Personal, Indoor and Mobile Radio Communications - (PIMRC), 2012, pp. 1565–1570, http://dx.doi.org/10.1109/PIMRC.2012.6362597, 1570.
[29] J. Marín Alfonso, JI. Martínez Torre, H. Arguello Fuentes, L.B. Agudelo, Compressive multispectral spectrum sensing for spectrum cartography, Sensors (Basel, Switzerland) 18 (2) (2018) 387, http://dx.doi.org/10.3390/s18020387, 29382145[pmid].
[30] D. Romero, S. Kim, R. López-Valcarce, G.B. Giannakis, Spectrum cartography using quantized observations, in: 2015 IEEE International Conference on Acoustics, Speech and Signal Processing, ICASSP, 2015, pp. 3252–3256, http://dx.doi.org/10.1109/ICASSP.2015.7178572, 3256.
[31] B.A. Jayawickrama, E. Dutkiewicz, I. Oppermann, G. Fang, J. Ding, Improved performance of spectrum cartography based on compressive sensing in cognitive radio networks, in: 2013 IEEE International Conference on Communications, ICC, 2013, pp. 5657–5661, http://dx.doi.org/10.1109/ICC.2013.6655495.
[32] B.A. Jayawickrama, E. Dutkiewicz, I. Oppermann, M. Mueck, Iteratively reweighted compressive sensing based algorithm for spectrum cartography in cognitive radio networks, in: 2014 IEEE Wireless Communications and Networking Conference, WCNC, 2014, pp. 719–724, http://dx.doi.org/10.1109/WCNC.2014.6952156.
[33] Y. Teganya, D. Romero, L.M.L. Ramos, B. Beferull-Lozano, Location-free spectrum cartography, IEEE Trans. Signal Process. 67 (15) (2019) 4013–4026, http://dx.doi.org/10.1109/TSP.2019.2923151.
[34] G. Zhang, X. Fu, J. Wang, X.L. Zhao, M. Hong, Spectrum cartography via coupled block term tensor decomposition, IEEE Trans. Signal Process. 68 (2020) 3660–3675, http://dx.doi.org/10.1109/TSP.2020.2993530.
[35] M. Hamid, B. Beferull-Lozano, Non-parametric spectrum cartography using adaptive radial basis functions, in: 2017 IEEE International Conference on Acoustics, Speech and Signal Processing, ICASSP, 2017, pp. 3599–3603, http://dx.doi.org/10.1109/ICASSP.2017.7952827.
[36] D. Romero, S. Kim, G.B. Giannakis, Stochastic semiparametric regression for spectrum cartography, in: 2015 IEEE 6th International Workshop on Computational Advances in Multi-Sensor Adaptive Processing, CAMSAP, 2015, pp. 513–516, http://dx.doi.org/10.1109/CAMSAP.2015.7383849.
[37] Y. Zhao, L. Morales, J. Gaeddert, K.K. Bae, J. Um, J.H. Reed, Applying radio environment maps to cognitive wireless regional area networks, in: 2007 2nd IEEE International Symposium on New Frontiers in Dynamic Spectrum Access Networks, 2007, pp. 115–118, http://dx.doi.org/10.1109/DYSPAN.2007.22.
[38] K. Ichikawa, T. Fujii, Radio environment map construction using hidden markov model in multiple primary user environment, in: 2017 International Conference on Computing, Networking and Communications, ICNC, 2017, pp. 272–276, http://dx.doi.org/10.1109/ICCNC.2017.7876138.
[39] C. Fan, X. Zhong, J. Wei, Bs-to-ground channel reconstruction with 3d obstacle map based on rss measurements, IEEE Access 7 (2019) 99633–99641, http://dx.doi.org/10.1109/ACCESS.2019.2930556.
[40] D. Huang, S. Wu, W. Wu, P. Wang, Cooperative radio source positioning and power map reconstruction: A sparse bayesian learning approach, IEEE Trans. Veh. Technol. 64 (6) (2015) 2318–2332, http://dx.doi.org/10.1109/TVT.2014.2345738.
[41] H. Idse, M. Hamid, T. Jordbru, L.R. Cenkeramaddi, B. Beferull-Lozano, Spectrum cartography using adaptive radial basis functions: Experimental validation, in: 2017 IEEE 18th International Workshop on Signal Processing Advances in Wireless Communications, SPAWC, 2017, pp. 1–4, http://dx.doi.org/10.1109/SPAWC.2017.8227752.
[42] H. Idse, M. Hamid, L.R. Cenkeramaddi, T. Jordbru, B. Beferull-Lozano, Experimental validation for spectrum cartography using adaptive multi-kernels, in: 2017 11th International Conference on Signal Processing and Communication Systems, ICSPCS, 2017, pp. 1–4, http://dx.doi.org/10.1109/ICSPCS.2017.8270459.
[43] S. Kim, G.B. Giannakis, Cognitive radio spectrum prediction using dictionary learning, in: 2013 IEEE Global Communications Conference, GLOBECOM, 2013, pp. 3206–3211, http://dx.doi.org/10.1109/GLOCOM.2013.6831565.
[44] D. Lee, D. Berberidis, G.B. Giannakis, Adaptive bayesian channel gain cartography, in: 2018 IEEE International Conference on Acoustics, Speech and Signal Processing, ICASSP, 2018, pp. 3554–3558, http://dx.doi.org/10.1109/ICASSP.2018.8461412.
[45] M. Angjelicinoski, V. Atanasovski, L. Gavrilovska, Comparative analysis of spatial interpolation methods for creating radio environment maps, in: 2011 19thTelecommunications Forum (TELFOR) Proceedings of Papers, 2011, pp. 334–337, http://dx.doi.org/10.1109/TELFOR.2011.6143557.
[46] K. Sato, T. Fujii, Kriging-based interference power constraint: Integrated design of the radio environment map and transmission power, IEEE Trans. Cogn. Commun. Netw. 3 (1) (2017) 13–25, http://dx.doi.org/10.1109/TCCN.2017.2653189.
[47] S. Üreten, A. Yongaçoğlu, E. Petriu, Interference map generation based on delaunay triangulation in cognitive radio networks, in: 2012 IEEE 13th International Workshop on Signal Processing Advances in Wireless Communications, SPAWC, 2012, pp. 134–138, http://dx.doi.org/10.1109/SPAWC.2012.6292873.
[48] J.D. Naranjo, A. Ravanshid, I. Viering, R. Halfmann, G. Bauch, Interference map estimation using spatial interpolation of mdt reports in cognitive radio networks, in: 2014 IEEE Wireless Communications and Networking Conference, WCNC, 2014, pp. 1496–1501, http://dx.doi.org/10.1109/WCNC.2014.6952411.

[49] M. Joneidi, H. Yazdani, A. Vosoughi, N. Rahnavard, Source localization and tracking for dynamic radio cartography using directional antennas, in: 2019 16th Annual IEEE International Conference on Sensing, Communication, and Networking, SECON, 2019, pp. 1–9, http://dx.doi.org/10.1109/SAHCN.2019.8824872.
[50] E. Dall'Anese, S. Kim, G.B. Giannakis, Channel gain map tracking via distributed kriging, IEEE Trans. Veh. Technol. 60 (3) (2011) 1205–1211, http://dx.doi.org/10.1109/TVT.2011.2113195.
[51] S. Debroy, S. Bhattacharjee, M. Chatterjee, Spectrum map and its application in resource management in cognitive radio networks, IEEE Trans. Cogn. Commun. Netw. 1 (4) (2015) 406–419, http://dx.doi.org/10.1109/TCCN.2016.2517001.
[52] A. Ben Hadj Alaya-Feki, B. Sayrac, S. Ben Jemaa, E. Moulines, Interference cartography for hierarchical dynamic spectrum access, in: 2008 3rd IEEE Symposium on New Frontiers in Dynamic Spectrum Access Networks, 2008, pp. 1–5, http://dx.doi.org/10.1109/DYSPAN.2008.35.
[53] Y. Zhao, J.H. Reed, S. Mao, K.K. Bae, Overhead analysis for radio environment map enabled cognitive radio networks, in: 2006 1st IEEE Workshop on Networking Technologies for Software Defined Radio Networks, 2006, pp. 18–25, http://dx.doi.org/10.1109/SDR.2006.4286322.
[54] S. Kim, E. Dall'Anese, G.B. Giannakis, Cooperative spectrum sensing for cognitive radios using 715 kriged kalman filtering, IEEE J. Sel. Top. Sign. Proces. 5 (1) (2011) 24–36, http://dx.doi.org/10.1109/JSTSP.2010.2053016.
[55] S. Alfattani, A. Yonzacoglu, Indirect methods for constructing radio environment map, in: 2018 IEEE Canadian Conference on Electrical Computer Engineering, CCECE, 2018, pp. 1–5, http://dx.doi.org/10.1109/CCECE.2018.8447654.
[56] D. Lee, S. Kim, G.B. Giannakis, Channel gain cartography for cognitive radios leveraging low rank and sparsity, IEEE Trans. Wireless Commun. 16 (9) (2017) 5953–5966, http://dx.doi.org/10.1109/TWC.2017.2717822.
[57] D. Romero, S. Kim, G.B. Giannakis, R. López-Valcarce, Learning power spectrum maps from quantized power measurements, IEEE Trans. Signal Process. 65 (10) (2017) 2547–2560, http://dx.doi.org/10.1109/TSP.2017.2666775.
[58] S. Sorour, Y. Lostanlen, S. Valaee, K. Majeed, Joint indoor localization and radio map construction with limited deployment load, IEEE Trans. Mob. Comput. 14 (5) (2015) 1031–1043, http://dx.doi.org/10.1109/TMC.2014.2343636.
[59] D.D. Ariananda, D. Romero, G. Leus, Cooperative compressive power spectrum estimation, in: 2014 IEEE 8th Sensor Array and Multichannel Signal Processing Workshop, SAM, 2014, pp. 97–100, http://dx.doi.org/10.1109/SAM.2014.6882349.
[60] H.B. Yilmaz, T. Tugcu, Location estimation-based radio environment map construction in fading channels, Wirel. Commun. Mob. Comput. 15 (2015) 561–570.
[61] D. Denkovski, V. Rakovic, M. Pavloski, K. Chomu, V. Atanasovski, L. Gavrilovska, Integration of heterogeneous spectrum sensing devices towards accurate rem construction, in: 2012 IEEE Wireless Communications and Networking Conference, WCNC, 2012, pp. 798–802, http://dx.doi.org/10.1109/WCNC.2012.6214480.
[62] Sandra Roger, Carmen Botella, Juan J. Pérez-Solano, Joaquin Perez, Application of radio environment map reconstruction techniques to platoon-based cellular v2x communications, Sensors 20 (9) (2020).
[63] V. Chowdappa, C. Botella, J.J. Samper-Zapater, R.J. Martinez, Distributed radio map reconstruction for 5 g automotive, IEEE Intell. Transp. Syst. Mag. 10 (2) (2018) 36–49, http://dx.doi.org/10.1109/MITS.2018.2806632.
[64] R.C. Dwarakanath, J.D. Naranjo, A. Ravanshid, Modeling of interference maps for licensed shared access in lte-advanced networks supporting carrier aggregation, in: 2013 IFIP Wireless Days, WD, 2013, pp. 1–6, http://dx.doi.org/10.1109/WD.2013.6686457.
[65] V. Icolari, D. Tarchi, A. Vanelli-Coralli, M. Vincenzi, An energy detector based radio environment mapping technique for cognitive satellite systems, in: 2014 IEEE Global Communications Conference, 2014, pp. 2892–2897, http://dx.doi.org/10.1109/GLOCOM.2014.7037247.
[66] G. Vanhoy, H. Volos, C.E.C. Bastidas, T. Bose, A spatial interpolation method for radio frequency maps based on the discrete cosine transform, in: MILCOM 2013-2013 IEEE Military Communications Conference, 2013, pp. 1045–1050, http://dx.doi.org/10.1109/MILCOM.2013.181.
[67] M. Angel Gutierrez-Estevez, R.L.G. Cavalcante, S. Stanczak, Nonparametric radio maps reconstruction via elastic net regularization with multi-kernels, in: 2018 IEEE 19th International Workshop on Signal Processing Advances in Wireless Communications, SPAWC, 2018, pp. 1–5, http://dx.doi.org/10.1109/SPAWC.2018.8445843.
[68] A. Kliks, P. Kryszkiewicz, Ł. Kułacz, Measurement-based coverage maps for indoor rems operating in tv band, in: 2017 IEEE International Symposium on Broadband Multimedia Systems and Broadcasting, BMSB, 2017, pp. 1–7, http://dx.doi.org/10.1109/BMSB.2017.7986162.
[69] Q. Wu, F. Shen, Z. Wang, G. Ding, 3D spectrum mapping based on roi-driven uav deployment, IEEE Netw. 34 (5) (2020) 24–31, http://dx.doi.org/10.1109/MNET.011.2000076.
[70] Y. Zhao, D. Raymond, C. da Silva, J.H. Reed, S.F. Midkiff, Performance evaluation of radio environment map-enabled cognitive spectrum-sharing networks, in: MILCOM 2007 - IEEE Military Communications Conference, 2007, pp. 1–7, http://dx.doi.org/10.1109/MILCOM.2007.4454765.
[71] Y. Zhao, J. Gaeddert, K. Bae, J. Reed, Radio environment map enabled situation-aware cognitive radio learning algorithms, 2006.
[72] S. Grimoud, S. Ben Jemaa, B. Sayrac, E. Moulines, A rem enabled soft frequency reuse scheme, in: 2010 IEEE GlobecomWorkshops, 2010, pp. 819–823, http://dx.doi.org/10.1109/GLOCOMW.2010.5700438.
[73] R. Mahapatra, E.C. Strinati, Interference-aware dynamic spectrum access in cognitive radio network, in: 2011 IEEE 22nd International Symposium on Personal, Indoor and Mobile Radio Communications, 2011, pp. 396–400, http://dx.doi.org/10.1109/PIMRC.2011.6139990.
[74] Z. Hou, Y. Zhou, L. Tian, J. Shi, Y. Li, B. Vucetic, Radio environment map-aided doppler shift estimation in lte railway, IEEE Trans. Veh. Technol. 66 (5) (2017) 4462–4467, http://dx.doi.org/10.1109/TVT.2016.2599558.
[75] C. Suarez-Rodriguez, Y. He, E. Dutkiewicz, Theoretical analysis of rem-based handover algorithm for heterogeneous networks, IEEE Access 7 (2019) 96719–96731, http://dx.doi.org/10.1109/ACCESS.2019.2929525.
[76] S. Contreras, G. Villardi, R. Funada, H. Harada, An investigation into the spectrum occupancy in japan in the context of tv white space systems, in: 2011 6th International ICST Conference on Cognitive Radio Oriented Wireless Networks and Communications, CROWNCOM, 2011, pp. 341–345, http://dx.doi.org/10.4108/icst.crowncom.2011.245857.
[77] Radiocommunications (low interference potential devices) class licence 2000, Australian communications and media authority, radiocommunications act, 2021.
[78] Daniel Denkovski, Vladimir Atanasovski, Liljana Gavrilovska, Janne Riihijärvi, Petri Mähönen, Reliability of a Radio Environment Map: Case of Spatial Interpolation Techniques, IEEE, 2012, http://dx.doi.org/10.4108/icst.crowncom.2012.248452.
[79] A.B.H. Alaya-Feki, S.B. Jemaa, B. Sayrac, P. Houze, E. Moulines, Informed spectrum usage in cognitive radio networks: Interference cartography, in: 2008 IEEE 19th International Symposium on Personal, Indoor and Mobile Radio Communications, 2008, pp. 1–5, http://dx.doi.org/10.1109/PIMRC.2008.4699911.
[80] C. Phillips, M. Ton, D. Sicker, D. Grunwald, Practical radio environment mapping with geostatistics, in: 2012 IEEE International Symposium on Dynamic Spectrum Access Networks, Vol. 795, 2012, pp. 422–433, http://dx.doi.org/10.1109/DYSPAN.2012.6478166.
[81] L. Bolea, J. Pérez-Romero, R. Agustí, Received signal interpolation for context discovery in cognitive radio, in: 2011 the 14th International Symposium on Wireless Personal Multimedia Communications, WPMC, 2011, pp. 1–5.
[82] L. Bolea, J. Perez-Romero, R. Agusti, O. Sallent, Context discovery mechanisms for cognitive radio, in: 2011 IEEE 73rd Vehicular Technology Conference, VTC Spring, 2011, pp. 1–5, http://dx.doi.org/10.1109/VETECS.2011.5956366.
[83] G. Mateos, J.-A. Bazerque, G.B. Giannakis, Spline-based spectrum cartography for cognitive radios, in: 2009 Conference Record of the Forty-Third Asilomar Conference on Signals, Systems and Computers, 2009, pp. 1025–1029, http://dx.doi.org/10.1109/ACSSC.2009.5470044.

[84] M. Angjelicinoski, V. Atanasovski, L. Gavrilovska, Comparative analysis of spatial interpolation methods for creating radio environment maps, in: 2011 19thTelecommunications Forum (TELFOR) Proceedings of Papers, 2011, pp. 334–337, http://dx.doi.org/10.1109/TELFOR.2011.6143557.
[85] I.A. Nalder, R.W. Wein, Spatial interpolation of climatic normals: test of a new method in the canadian boreal forest, Agricult. Forest Meteorol. 92 (4) (1998) 211–225, http://dx.doi.org/10.1016/S0168-1923(98)00102-6.
[86] R. Mahapatra, E.C. Strinati, Interference-aware dynamic spectrum access in cognitive radio network, in: 2011 IEEE 22nd International Symposium on Personal, Indoor and Mobile Radio Communications, 2011, pp. 396–400, http://dx.doi.org/10.1109/PIMRC.2011.6139990.
[87] H.B. Yilmaz, T. Tugcu, Location estimation-based radio environment map construction in fading channels, Wirel. Commun. Mob. Comput. 15 (3) (2015) 561–570.
[88] G. Sun, J. van de Beek, Simple distributed interference source localization for radio environment mapping, in: 2010 IFIP Wireless Days, 2010, pp. 1–5, http://dx.doi.org/10.1109/WD.2010.5657755.
[89] E. Meshkova, et al., Experimental spectrum sensor testbed for constructing indoor radio environmental maps, in: 2011 IEEE International Symposium on Dynamic Spectrum Access Networks, DySPAN, 2011, pp. 603–607, http://dx.doi.org/10.1109/DYSPAN.2011.5936253.